[SSC23-WVIII-07]

# Development of a $KMNO_4$ Catalyst-Infused Fuel Grain for H2O2 Hybrid Thruster Ignition Enhancement

Ryan Thibaudeau, Stephen A. Whitmore
Department of Mechanical and Aerospace Engineering, Utah State University
Logan, Utah 84322; 651-278-9756
ryan.j.thibaudeau@gmail.com

## ABSTRACT

Utah State University's patented High Performance Green Hybrid Propulsion (HPGHP) technology leverages unique dielectric breakdown properties of 3D-printed acrylonitrile butadiene styrene (ABS), allowing re-start, stop, and re-ignition. HPGHP works most reliably using gaseous oxygen (GOX) as the oxidizer but has experienced ignition reliability and latency issues when replaced high test hydrogen peroxide (HTP), which has a significantly higher storage density. This deficiency results from HTP's high decomposition energy barrier. Traditionally, inline external catalyst beds or GOX pre-lead burns are used to overcome this energy barrier to achieve ignition; however, the extra hardware required for these systems have inhibited their adoption into flight units for small satellite propulsion modules. The presented research replaces the external catalyst by diffusion-blending ABS with 1-2% potassium permanganate ($KMNO_4$), and then 3-D printing fuel grains using the augmented feed-stock. The embedded catalyst allows for near-instantaneous decomposition as HTP enters the combustion chamber, releasing gaseous oxygen that, when combined with the arc-ignition energy, provides quick and reliable ignition. No preheat is required, and the infused fuel does not reduce the overall system performance. "Drop-in" design options and test results are presented for a prototype system at a1 N thrust level using 90% HTP.

## INTRODUCTION

Significant advances in the miniaturization of electronic components have emerged during the first two decades of the 21st century and have allowed spacecraft bus sizes to shrink by nearly an order of magnitude. Spacecraft as small as 25 kg now offer the sensing and computational capability of a spacecraft weighing more than several hundred kilograms from just a generation ago. As a result, global interests in very small spacecraft (SmallSats) have grown dramatically, and a competitive commercial market has emerged during the last decade.

To date, SmallSats have primarily been used for educational, technology demonstration, or other novelty purposes. SmallSats are currently launched using a limited number of "ride-share" options that rely on the excess launch vehicle payload capacity. These ride-share options offer secondary payload satellite customers little or no control over the launch schedule and the achieved final orbit. To support the expending capability of SmallSats, a cheap, reliable, high-performing, safe, and preferably, "green" propulsion unit is required in order to re-position the spacecraft properly; and once-inserted, maintain the required orbit. Figure 1 shows the current state of CubeSat propulsion systems with flight heritage. Unfortunately, SmallSat technology development has primarily centered on spacecraft bus design and miniaturization of sensor components. Generally, the propulsion industry has not kept pace with the bus avionics growth trend. With the current state of the art only a few space propulsion options are available to the systems designer.

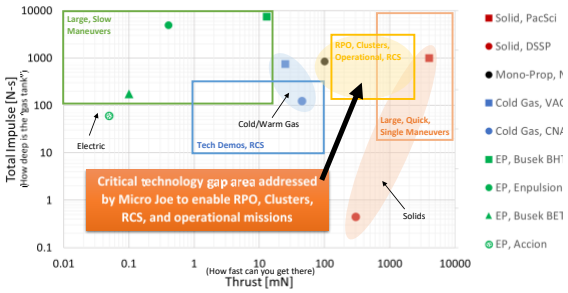


**Figure 1. Current SmallSat Propulsion Trade space.**

This lack of options is insufficient to support the emerging growth demands of the "NewSpace" economy.

The cost associated with these propulsion systems has led to many small satellites launching with no propulsion: often restricting the capability of the mission. In support of the SmallSat market demands, the hybrid propulsion system discussed in this paper aims to address two key issues in filling the technology gap shown in Figure 1, handling safety and the prohibitive

cost requirement that often impeded SmallSat developers from incorporating propulsion into their design.

## BACKGROUND

This section describes the properties of hydrazine and the hazards and environmental issues associated with its use. Next the emerging class of green propellants based on ionic-liquids is described, and the associated environmental and operational issues are described. Finally, hybrid rocket systems using environmentally friendly propellants are offered as a potential solution. Issues associated with their operational use are presented.

### *Hydrazine as the Current Operational Standard for In-Space Propulsion.*

Hydrazine is a very effective and reliable monopropellant. Hydrazine thrusters are simple, versatile, and dependable. Hydrazine technology has been under development since the late 1950's and has a very high technology readiness level (TRL) level.

Unfortunately, hydrazine-based systems bring a wide range of objective and environmental hazard issues. Hydrazine is a highly toxic and dangerously unstable substance. The United States Environmental Protection Agency classifies hydrazine as "highly toxic." Hydrazine is destructive to living tissues and is a known carcinogen.[1] Hydrazine possesses a high vapor pressure and boils readily at room temperature. Thus, there exists significant risk of respiratory contamination, and special servicing procedures that employ full-pressure self-contained atmospheric protective ensemble suits are required. The toxicity and explosion potential of hydrazine requires extreme handling precautions.

### *On the Need for a "Green" Replacement for Hydrazine as a Spacecraft Propellant.*

With a growing regulatory burden, the associated infrastructure requirements for hydrazine transport, storage, servicing, and clean up resulting from accidental releases, are rapidly making the use of hydrazine cost prohibitive. A recent study by the European Space Agency Space Research and Technology Center (ESTEC)[2,3] identified *"reduced production, operational, and transport costs associated with lower propellant toxicity/explosion hazards...,"* as an essential operations change required for achieving low-cost commercial space access developing a non-toxic, stable "green" alternative for hydrazine was highly recommended.

In response to this recommendation, The USAF,[4] NASA,[5] and the Swedish Space Corporation Ecological Advanced Propulsion Systems (ECAPS) [6] are actively involved in the development of green alternatives to hydrazine. A useful "green" replacement for hydrazine must be sufficiently chemically and thermally stable to allow technicians and engineers to safely work with the propellant in a normal "shirt-sleeve" commercial environment; but must reliably combust and have good performance properties. Cryogenic or high freezing point propellants requiring temperature control are not appropriate for space propulsion applications. Although mass-specific impulse is important, volume-specific impulse *(density impulse)* is an even more important consideration, and a high propellant storage density is preferred.

### *Ionic Liquids as an Alternative to Hydrazine*

Although some low-TRL electrical-chemical systems in SmallSat scales have been tested[7], currently the only operational green chemical-propellant options are associated with the ionic-liquids (ILs)[8] Ammonium Dinitramide (ADN),[9,10,11,12] and Hydroxyl Ammonium Nitrate (HAN).[13,4 ,14] Both propellants have achieved at least one spaceflight, with the ADN-based propellant LMP-103S flying on the PRISMA Spacecraft,[15] and the HAN-based propellant AFM-315E flying on NASA's Green Propellant Infusion Mission (GPIM)[16,17] The PRISMA flight report[18] states that LMP-103S delivered equivalent–to-superior performance to hydrazine, with a vacuum specific impulse of 230 seconds. The GPIM flight report does not specifically report the achieved in-flight specific impulse ($I_{sp}$) for AFM-315E, but extrapolations from ground tests show that $I_{sp}$ values between 220 and 230 seconds are achievable[17].

### *Environmental and Operational Issues Associated with Ionic Liquid Propellants*

In spite of being called "green," by their manufacturers, IL-based propellants are generally not environmentally-friendly. Both of the above-mentioned IL-propellants are toxic to organic tissue, for example AF-M315E contains hydroxyethyl hydrazine (HEHN) as an ignition enhancer and burn stabilizer. In in high concentrations IL-based propellants are prone to energetic uncontrolled decomposition events. Thus, special handling precautions are required for processing and storage. The major advantage of both propellants is a low-vapor pressure at room temperature, allowing handling and

servicing without the use of Self Contained Atmospheric Protective Ensemble (SCAPE) suits.

Because of these properties, the USAF has recently begun to refer to such IL-formulations more properly as having "reduced toxicity" instead of being "green." In addition to potential toxicity and objective hazards, there exist several key developmental issues that make IL-based propellants unsuitable for some small spacecraft applications.

The high water content makes *IL*-propellants notoriously hard to ignite,[19] and LMP-103S and AFM-315E propellants cannot be cold-started. Multiple catalyst systems have been developed to augment IL ignitability; however, the associated catalyst beds must be preheated from 350-400ºC before and during ignition. This pre-heat cycle pre-heat consumes a significant amount of energy. For example, on the Prisma[15] demonstration flight the pre-heat time was 30 min, requiring 16.7 kJ of total energy input. This input was required for every cold-cycle of the LMP-103S thruster. Thus, it can be concluded that the ionic liquid catalyst beds and associated heating systems add significantly to the inert mass of the spacecraft and the high-wattage preheat requirement presents a significant disadvantage for small spacecraft where power budgets are extremely limited.

Also, due to the very slow reaction kinetics demonstrated by Hori and Katsumi[20] for HAN, and Whitmore and Burnside[21] for ADN at the moderate pressures levels required for SmallSat Thruster systems (1000–2000 kPa), ignition latencies can be significant, up to several seconds, and may limit the usefulness of IL-propellants for spacecraft maneuvering and control systems. Below 1000 kPa chamber pressure the IL liquid propellants will not ignite, and this issue limits the ability to scale these systems for thrusters below the 1-N thrust level.

Clearly, significant technology improvements must occur before IL-based systems can be employed as a primary propulsion unit or as part of the reaction control system for small spacecraft. With the current state of propulsion technology, the only proven non-hazardous propulsion alternative to hydrazine, and available for small ride-share payloads, is based on low-performing cold-gas thrusters.

Even under ideal operating conditions, when compared to conventional solid, hybrid, or bi-propellant options, the performances of ionic liquid propellants are generally quite low — with achieved vacuum $I_{sp}$ values at or less than 230 seconds. The combination of these middling performance characteristics and lack of truly "green" advantages have led some in the industry to question whether ionic liquids as propellants have been "oversold".[22] Clearly, significant technological issues exist and must be overcome before the ionic-liquid propellants are used routinely as a hydrazine replacement.

***Hybrid Rockets as Green Alternative for In-Space Propulsion.***

In response to this emerging need for environmentally-sustainable in-space propulsion systems, hybrid rocket systems have emerged as a potential alternative to traditional toxic-propellants. When compared to conventional liquid- and solid- propelled rocket systems, hybrid rockets possess well-known operational safety and handling-advantages. A study by the U.S. Department of Transportation concluded that hybrid rocket motors can be safely stored and operated without a significant risk of explosion or detonation and offer the potential to significantly reduce operating costs for commercial launch vehicles.[23] Finally, Hybrid rocket systems offer higher performance than hydrazine-based systems; and their inherent-design safety offers a significant potential for ride-share spacecraft applications.

***Operational Issues Associated with Hybrid Rockets***

However, in spite of these well- known safety and handling advantages; conventionally-designed hybrid rocket systems have not seen widespread commercial use due to two key technical challenges. The first technical challenge is the current lack of an operational method reliable multiple-use ignition, allowing on-demand start, stop, and re-start. The second technical challenge is low fuel regression rates associated with hybrid combustion.

Because of the relative propellant stability, hybrid rocket systems can be difficult to ignite; and a substantial ignition enthalpy source is required. The ignition source must provide sufficient heat to pyrolize the solid fuel grain at the head end of the motor, while simultaneously providing sufficient residual energy to overcome the activation energy of the propellants. Such high-energy devices often come with a suite of environmental and objectives risks, and operational challenges.

Most conventional hybrid rocket applications have used high output pyrotechnic or "squib" charges to initiate combustion. Pyrotechnic charges are extremely susceptible to inadvertent detonation due to with electromagnetic radiation,[24,25] and present significant explosion hazards that are incompatible with rideshare opportunities. Most importantly, for nearly all applications pyrotechnic ignitors are designed as "one-shot" devices that do not allow a multiple restart capability. Thus, the great potential for restartable upper stages or in-space maneuvering systems using hybrid propulsion has remained largely unrealized. An operational hybrid system with multiple restart capability does not currently exist.

The second disadvantage is that the internal motor ballistics of hybrid combustion produce regression rates that are typically between 30 and 40% of the regression rates of solid fuel motors of the same thrust and impulse class.[26,27] To make up for the lower regression rate, a higher oxidizer mass flow rate is required to maintain the same thrust level. This increases the system's oxidizer-to-fuel (O/F) ratio and ultimately results in poor mass impulse performance, erosive fuel burning, nozzle erosion, reduced motor duty cycles, potential combustion instability, and poorer overall performance of the system. To overcome this O/F problem, hybrid rockets are traditionally designed with cylindrical fuel ports that have high length-to-diameter ratios. This high aspect ratio can result in poor volumetric efficiency, and thus limits a hybrid motor application to a customarily volume-constrained small satellite.[28]

### *High Performance Green Hybrid Propulsion Systems*

In order to fill the technology gaps as described in the previous section, over the past decade Space Dynamics Laboratory (SDL) and the Propulsion Research Laboratory at Utah State University (PRL-USU) have actively teamed to develop a High Performance Green Hybrid Propulsion (HPGHP) technology as a safe and environmentally-sustainable replacement for hydrazine across a wide range of applications.

HPGHP is enabled by recent advances in 3D printing and leverages unique electrical breakdown characteristics of certain 3D-printed plastics, the most effective being acrylonitrile butadiene styrene (ABS). Additive manufacturing changes the electrical breakdown properties, and when printed materials are presented with an inductive electrical potential, electrical-arcing along the layered surface pyrolyzes material and seeds combustion when an oxidizing flow is introduced.[29] This "sparking" property has been developed into a proprietary, power-efficient system that can be cold-started and restarted with a high degree of reliability. Multiple prototype units with thrust levels varying from less than 1 N to greater than 900 N have been developed and tested.[30,31,32]

Although there may appear to be some similarities, the arc-ignition method described in this paper is distinctly different from the action of a pulse plasma thruster[7]. Pulse plasma thruster designs use a high alternating current source to pyrolyze the surface of a Teflon block. The high current in the plasma arc induces a magnetic field. The action of the current and the magnetic field causes the plasma to be accelerated. When the current is stopped, pyrolysis ceases. A typical ignition cycle requires up to 1 kW of power. The arc-ignition method used in this work requires a low direct current source to pyrolyze the fuel material. Additive printing of the fuel changes the material dielectric proper ties; when ABS is subjected to the electro- static potential between embedded electrodes, the layered structure allows an "arc track" to be carved between the electrodes. Associated joule heating pyrolyzes the fuel; and as oxidizing flow is introduced, ignition spontaneously occurs. Combustion continues even after the current source is terminated. A typical ignition cycle requires less than 5 W of power applied for less than a second, and consumes less than 5 joules of total ignition energy. Once started, the system can be sequentially fired with no additional energy inputs required. Figure 2 shows a schematic of the HPGHP Ignition System Electronics, and Figure 3 shows the head-end of a 3D-printed ABS

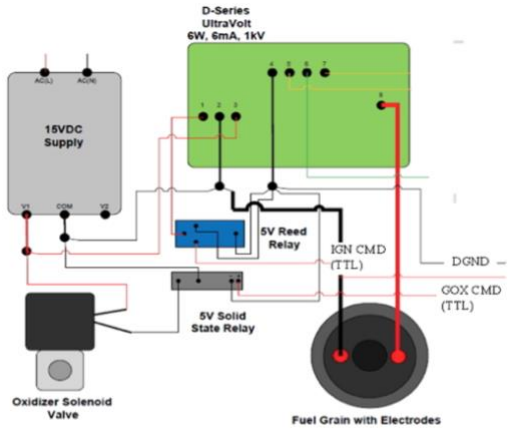


**Figure 2. Ignition System Electronic Schematic.**

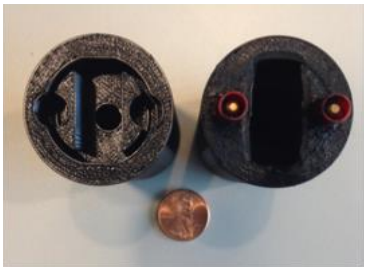

**Figure 3. 3D Printed Fuel Grain with ESC-Terminated Electrodes.**

fuel grain with embedded electrodes.

The patented system[33] has been scaled over a large range with successful prototypes with thrust levels varying from 5 to 900 N having been tested.[7] Multiple oxidizers including gaseous oxygen (GOX), nitrous oxide ($N_2O$), hydrogen peroxide ($H_2O_2$), enriched air (EAN40), and Nytrox have been successfully tested with the HPGHP system. Nytrox is a "green" blend GOX and $N_2O$ and is similar to the laughing gas used for medial anesthesia

applications. A flight-weight 25 N thruster system was extensively vacuum tested.[34]

On 25 March 2018, a flight experiment containing a 10 N prototype of this thruster system was launched aboard a two-stage Terrier-Improved Malemute sounding rocket from Wallops Flight Facility. The launch achieved apogee of 172 km, allowing more than 6 min in a hard-vacuum environment above the Von-Karman line. The thruster was successfully fired five times Whitmore and Bulcher[35] report the results of this flight test experiment.

### *On the Need for Higher-Density Hybrid Oxidizers*

In its most mature form, the HPGHP system uses GOX as the oxidizer with 3D-printed ABS as the fuel. The GOX/ABS propellants are highly mass efficient system, with a flight weight 25 N thruster system achieving vacuum $I_{sp}$ greater than 300 seconds. Unfortunately, unless stored at very high pressures, GOX has a low specific gravity and is a volumetrically inefficient propellant.

Due to its high density, hydrogen peroxide was considered to be very promising alternative oxidizer for this application. In order to achieve comparable density to $H_2O_2$, GOX would need to be stored at pressures above 10,000 psi. When using a 90% hydrogen peroxide solution as an oxidizer along with a thermoplastic fuel in a hybrid system, there exists the potential for performance at a very high level. Table 1 compares the performance of a hypothetical 90% peroxide/ABS system to hydrazine, LMP-103S and AFM315-E. This work has investigated using an aqueous solution of 90% $H_2O_2$, as a "drop-in" replacement for GOX in the HPGHP system. Data for hydrazine, LMP-103S and AFM315-E were taken from Ref. [4].

### *Issues Associated with Catalytic Ignition of $H_2O_2$ in Hybrid Motors*

Although HPGHP ignition works quite reliably using GOX as the oxidizer; HPGHP has experienced reliability and ignition latency issues when replaced by hydrogen peroxide. The reasons for these issues will be described in the following sections. High concentrations of 90% or greater of hydrogen peroxide, referred to as high-test peroxide (HTP), have been used extensively for propulsion applications, both as a monopropellant and in combinations with fuels. Figure 4 shows the associated end-to-end reaction. In this reaction both oxidation and reduction occur at the same time. This reaction is very energetic producing up to 98.1 kJ for every mole of peroxide that is decomposed (3.33 MJ/kg). Typically, an aqueous solution of HTP is sufficiently stable to work with, requiring an activation energy of approximately 75 kJ/mol in the absence of a catalyst. Figure 5 shows this transition process.

In typical rocket applications with $H_2O_2$ as a monopropellant, a heated catalyst bed is used to initiate decomposition. The catbed lowers the activation energy to the point where a moderate amount of heat can initiate decomposition. Noble metal catalysts like platinum or silver can lower the activation energy to less than 50 kJ/mol. Although catalytic decomposition of monopropellant HTP has been successfully used for a variety of applications, this method typically requires very high concentrations of peroxide, greater than 90%. Even then, "wet" partially decomposed burns are very

**Table 1. Comparison of Performance Characteristics.**

| **Propellant** | **Hydrazine** | **LMP-103S** | **AF-M315E** | **$H_2O_2$/ABS Hybrid** |
|---|---|---|---|---|
| Flame Temperature | 600-750$^o$C | 1600 $^o$C | 1900$^o$C | 2900 $^o$C |
| $I_{sp}$, *sec* | 220-225 | 252 (theory),<br>235 (delivered) | 266 (theory)<br>245 (delivered) | 324 (theory)<br>302 (delivered) |
| Specific Gravity | 1.01 | 1.24 | 1.465 | 1.392 (90% $H_2O_2$) |
| Density Impulse, *N-sec/liter* | 2270 | 3125 (theory)<br>2915 (delivered) | 3900 (theory)<br>3650 (delivered) | 4450 (theory)<br>4002 (delivered) |
| Preheat Temperature | 315$^o$C, cold-start capable | 300$^o$C | 370 $^o$C | N/A<br>none-required |
| Required Ignition Input Energy, *Joules* | N/A | 18,000 J (10 Watts @ 1800 seconds) | 27,000 J (15 Watts @ 1800 seconds) | 2-8 J (8-16 Watts for 250-500 msec) |
| Propellant Freezing Temperature | 1-2$^o$C | -7$^o$C | < 0$^o$C *(forms glass, no freezing point)* | -10$^o$C *(90% concentration)* |
| Cost | $$$ | $$$ | $$$$ | $ |
| Availability | Readily Available | Restricted Access | Limited Access | Very Widely Available[i] |
| NFPA 704 Hazard Class |  |  | 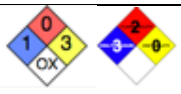 |  |

typical. As shown by Figure 4, even in fully decomposed HTP plumes, water is an inherent by-product.

When catalytic decomposition is applied to hybrid rocket systems, the results are less satisfactory. As the oxidizer plume exits the injector and enters the hybrid combustion


**Figure 4. Hydrogen Peroxide Decomposition Reaction.**

chamber, it rapidly expands and super-cools to well below the evaporation temperature of water. As a result, liquid water re-condenses and the "soaked" fuel grain will simply not ignite. This problem appears to be endemic to all hybrid rockets but is especially problematic when lower concentration peroxides (<90%) are used.

The ESA-funded Nammo Raufoss Project[36] has been ongoing since 2003 and is currently the most accomplished of the existing peroxide-hybrid programs. The Nammo design used HTPB as the accompanying fuel. For this design the peroxide solution was decomposed using SAAB's proprietary catalyst bed design, with the resulting hot gasses injected into the combustion chamber through a vortex injector. The catalyst bed hybrid was able to work with peroxide concentrations as low as 87.5%, but the catbed was quite large and made up a considerable fraction of the overall inert motor weight.

For the typical Nammo motor ignition sequence, after peroxide flow is initiated the chamber pressure gradual builds up from ambient to a plateau at approximately 1500 kPa (220 psia). This "smoldering" buildup of chamber pressure takes slightly more than 2 seconds, followed by a sharp rise in chamber pressure to approximately 2500 kPa bars (360 psia). NAMMO refers to the initial pressure buildup as the "*mono-propellant combustion mode*." and the sharp rise and subsequent plateau as "*hybrid combustion mode*."

As reported by Whitmore and Merkley (2017)[37] no matter the concentration level, the initial expansion from the catbed exit to ambient will always super-cool the water vapor in the decomposition products and result in a "wet motor." This expansion and adiabatic cooling phenomenon is very likely the reason for the large ignition latencies and the self-described "*monopropellant*" combustion modes, smoldering burns, and large ignition latencies experienced by the NAMMO hybrid motors. In any case, the resulting enthalpy levels are often too low to achieve full combustion, and ignition is highly unreliable.

It must be noted that, in addition to the previously-

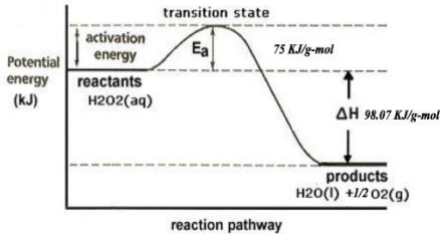


**Figure 5. Peroxide Decomposition Energy State.**

described ignition reliability issues, catalyst beds also pose a series of operational issues:

- Catbeds are heavy and volumetrically inefficient. They contribute nothing to the propulsive mass of the system.
- In order to be effective, catalysts must be externally heated to high temperatures, often exceeding 300°C. As described previously, this pre-heat presents a serious problem for SmallSats that have limited energy budgets.
- Catbeds often self-consume at the high temperatures necessary for efficient decomposition action,
- Catalyst beds can be "poisoned" and rendered ineffective in the presence of stabilizers in HTP.

Because $H_2O_2$ catbeds tend to rely on noble metals like silver or platinum as the active agent, they are extremely expensive, and the final two events in the above list can significantly increase programmatic development costs.

### *Catalytic Assist for Arc-Ignition of $H_2O_2$ in Hybrid Motors.*

Previous studies by Whitmore and Martinez[38,39] have demonstrated that a catalytic-assist, where a catalyst bed is placed in line with the system, significantly increases ignition reliability and reduces ignition latency. Catalytic-assist works by partially decomposing the incoming oxidizer to release free oxygen before entering the combustion chamber. Because catalytic-assist is only intended to assist the arc ignition system, and not fully decompose the incoming HTP; pre-heat is not required, and far less expensive materials like potassium permanganate, manganese dioxide, manganese (III) oxide, and potassium nitrate can be used in lieu of silver and platinum.

### *Thermal Decomposition of $H_2O_2$ Using GOX Pre-Lead and Pre-Ignition*

Even with the success of the previously described

catalytic-assist methods, considering the issues associated with catbeds, including weight and volume, it is desirable to remove the catalytic system entirely from the design. An alternative method initiates combustion using a gaseous oxygen pre-lead and then introduces HTP to the hot combustion chamber. Residual energy from the GOX/ABS combustion thermally decomposes the HTP flow, with the freed oxygen allowing full hybrid combustion to initiate.

Previously, this thermal ignition method was applied by Whitmore[40] for ignition of a larger-76 mm, 140 N thrust hybrid system. Thermal decomposition for an HTP-hybrid on the proposed 1 N to 5 N thrust level required for SmallSat propulsion was investigated by Smith[46]. While he saw success with this method, there are still drawbacks for this system; 1) System architecture doubles in complexity because separate plumbing, valves, and sensors are needed for the GOX lines. 2) Spacecraft volume is sacrificed because transitioning from a ground-based developmental unit to a space-ready flight unit requires a high pressure GOX tank and its associated plumbing and controls, which don't directly contribute to the propulsion system's power or efficiency. The smaller the spacecraft is, the greater the percent volume increase, making the drawback more significant. For a spacecraft classified as a Small Satellite, this approach is not viable to allow for enough HTP propellant to be stored onboard to achieve a delta-V that's useful for most space missions.

## THEORETICAL CONSIDERATIONS

This section discusses three key considerations that were investigated during this preliminary testing campaign. These considerations are 1) the effects of Oxidizer-to-Fuel Ratio (O/F) and fuel grain geometry on motor performance, 2) assessing the potential for motor feed-coupling instability, and 3) the effect of infusing catalyst material into the fuel grain and igniter to improve ignition latency and reliability.

### *Effects of O/F Ratio and Fuel Grain Geometry on Motor Performance.*

Hybrid Rocket systems generally favor a narrow range of O/F ratios where the system performance is near optimal. Figure 6 illustrates this point where the characteristic velocity $c_*$ and Vacuum $I_{sp}$ of two different 3D-printable fuels, ABS and polymethylmethacrylate

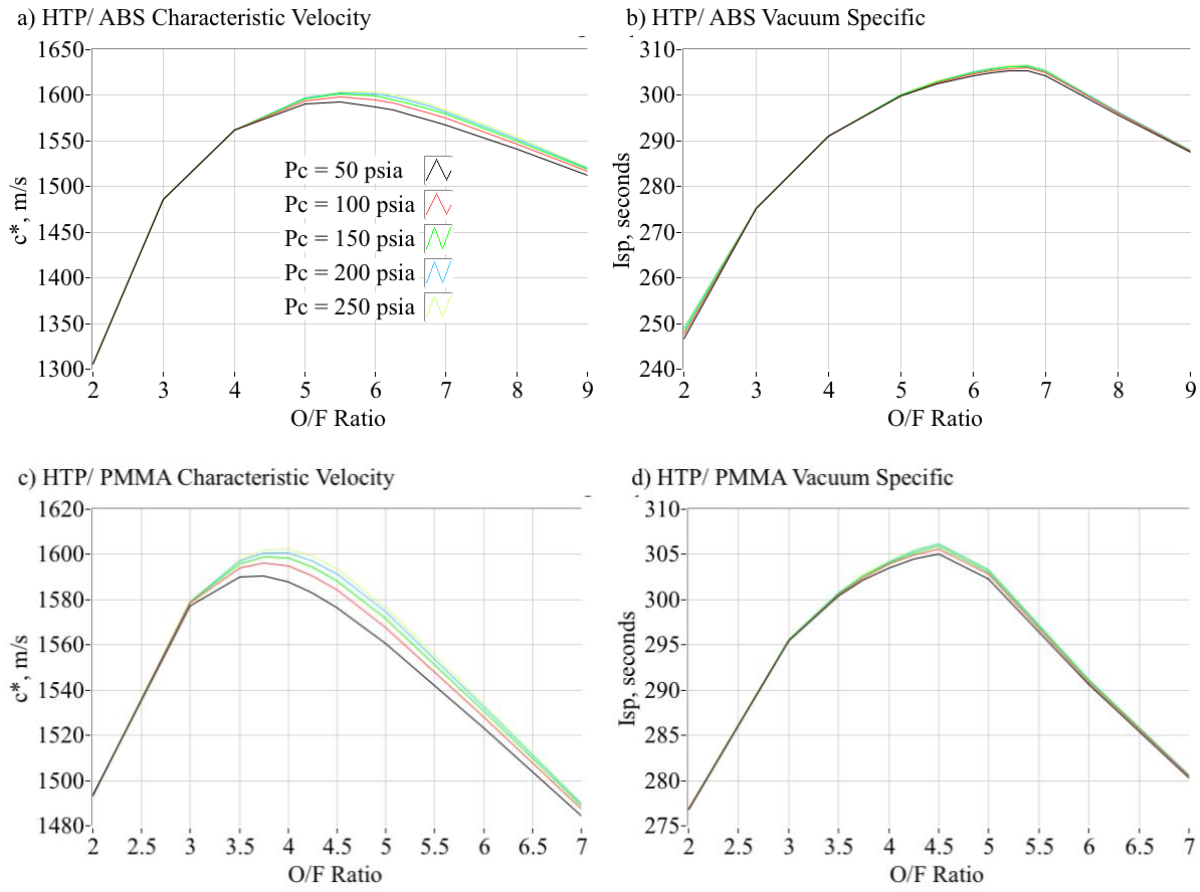


**Figure 6. Theoretical Performance Comparison of Two 3D Printed Hybrid Rocket Fuels as Burned with 90% HTP.**

(PMMA),[i] burned with 90% aqueous $H_2O_2$ are plotted as a function of O/F ratio for 5 different chamber pressures, 50, 100, 150, 200 and 250 psi. These calculations were performed using the NASA industry-standard chemical equilibrium code CEA,[41] and assume a 25:1 nozzle expansion ratio for the specific impulse calculation. Note that, although the fuels exhibit similar $c^*$ and Vacuum $I_{sp}$ levels, the optimal point for ABS occurs at a considerably higher O/F ratio, when compared to PMMA.

Generally, it is observed that the primary heat-transfer mechanism for fuel pyrolysis in larger-scale hybrid rocket systems forced convection within the boundary layer, Sutton and Biblarz (Ref. [26, Chapt. 11]). As the fuel port opens, greater burn area is exposed and this growth in burn area is greater than the drop-off in fuel regression rate resulting from the drop in oxidizer massflux. The result is that the large majority of hybrid rockets tested to date tend to experience oxidizer-to-fuel ratios that shift from fuel-rich to lean during the burn lifetime. Fuel regression rates are only weakly dependent on motor size.

In contrast, at small scales, i.e., 5 N thrust levels and lower, oxidizer massflux is sufficiently small that the rate of convective heat transfer is significantly reduced. For this combustion regime, radiative heat transfer dominates fuel pyrolysis. Whitmore and Merkley[42] have shown that unlike massflux-driven fuel regression for larger hybrid systems, the radiation-driven fuel regression rates of small-scale hybrids tend to grow with time. As a result, small-scale hybrids tend to burn with a reverse behavior, from shifting from lean to fuel-rich over the burn lifetime.

Thus, at small scales low hybrid fuel-regression rates are not an issue. In fact, the reverse behavior is experienced. In order to keep fuel regression rates near the optimal points one must anticipate this O/F shift and design the system to initially burn very lean, with the O/F shift crossing over the optimal point.

Although Figure 6 shows that both propellant sets achieve above 300 seconds theoretical vacuum $I_{sp}$, this range is rather narrow and drops off rapidly as the motor burns rich. Due to the tendency of small-scale hybrids to burn richer with time, this result has significant ramifications with respect to the real-world motor performance.

It must be noted that previous small thruster tests[43] with GOX/ABS and GOX/PMMA propellants have demonstrated that PMMA fuel results in a considerably lower fuel regression rate with a smaller overall O/F shift. This more constant O/F shift is of a considerable advantage for systems with long burn lifetime. For comparison purposes both fuels were burned with HTP in this testing campaign. Those comparisons will be presented later in the Results and Discussion section of this paper.

### *Assessing the Potential for Injector Feed Coupling*

Because HTP is highly incompressible, there exists a strong potential for injector-feed coupling during hybrid combustion. As described by Karabeyoglu et al.,[44] the underlying dynamics of the injector system is governed by the inertia of the fluid mass in the injector orifice and the pressure difference between the injector manifold and the combustion chamber. As derived by Sutton and Biblarz (Ref. [26, Chapt. 6]), the incompressible massflow of HTP through the injector and into the combustion chamber can be modeled using the classical discharge area model,

$$\dot{m}_{HTP} = C_D \cdot A_{inj} \sqrt{2 \cdot \rho_{HTP} \cdot \left( p_{inj} - p_{chamber} \right)} \quad . \quad (1)$$

In Eq. (1) $C_D \cdot A_{inj}$ is the injector discharge area, $\rho_{HTP}$ is the oxidizer fluid density, $p_{inj}$ is the injector feed pressure, and $p_{chamber}$ is the motor head end chamber pressure. Because the massflow through the injector port depends on both the injector feed pressure and the motor chamber pressure, there is a feedback mechanism that can lead to injector-coupling instability.

Injector feed coupling results in a low-frequency instability, that generally lies between 10 and 25 hertz. This oscillation results when the burn process is perturbed, resulting in a transient increase on chamber pressure, this increase subsequently drops the massflow rate into the chamber, resulting in a lowered fuel burn rate, and a subsequent drop in chamber pressure. The chamber pressure drop increases the massflow, and the cycle repeats. Depending on the motor geometry and the combustion rates of the propellants, feed-coupling instability can be mild or severe. A key driver of severe instability is combustion delay caused by slow vaporization of the incoming oxidizer.

To mitigate the potential coupling instability, a commercial atomizing 45° cone-spray nozzle[ii] was used. It was considered that a straight-port injector, which shoots a stream of liquid HTP directly into the fuel port and the flame zone offered the highest potential for injector-feed coupling. The atomizing cone-spray nozzle was intended to break up and spread the injected HTP,

[i] It must be noted that the method of 3D-printed for ABS is fused deposition manufacturing (FDM), and the printing method for PMMA is UV-Cure or Polyjet. ®

[ii] Snow performance, "Boost Cooler Water Injection Nozzle, Size 1-60 ml, https://www.snowperformance.eu/en/water-injection/boost-cooler-water-methanol-nozzle-sno-n0100. [Accessed 28 May 2022]

resulting in faster evaporation, thereby buffering any potential feed coupling instabilities.

***Potential for a Catalyst-Infused Fuel Grain***

Preliminary tests, shown later in this paper, indicate that potassium permanganate ($KMnO_4$) can be heterogeneously infused into a 3D printed ABS shell, significantly enhancing ignition-reliability without adversely affecting the overall system performance. Here the infused catalyst initiates HTP oxidizer decomposition upon contact, releasing oxygen gas and enabling the effectiveness of the arc-ignition system. Because infused catalyst directly releases oxygen in the combustion chamber, the need for an external catbed or thermal pre-lead is eliminated. Test data for this catalyst-infused fuel grain (CatGrain) is presented later.

## DATA ANALYSIS METHODS

This section details the analytical methods that were used to calculate key derived parameters from the raw test data. These mass-flow based calculations include 1) oxidizer massflow, 2) total massflow exiting the nozzle, 3) fuel massflow, 4) oxidizer-to-fuel ratio. Key performance parameters calculated from the raw data include 1) combustion efficiency, 2) thrust coefficient, 3) specific impulse, 4) characteristic velocity, and 5) impulse density. The following section details how these calculations were performed.

***Calculating the Fuel Massflow Rate.***

Although the inline Venturi measures the oxidizer massflow in real-time, the test stand was not configured to directly measure the fuel massflow. Instead, before and after each hot-firing the fuel grains were weighed to give the total fuel mass consumed during the test. As will be described later in this section, these mass measurements were used to anchor the "instantaneous" fuel massflow rates, calculated as the difference between the nozzle exit and oxidizer massflows,

$$\dot{m}_{fuel} = \dot{m}_{total} - \dot{m}_{ox} . \tag{2}$$

Knowing the nozzle throat area $A^*$ and the plume exhaust gas properties, the nozzle exit (total) massflow at each time point was calculated from the measured chamber pressure time history $P_0$, using the 1-dimensional choking massflow equation, [Anderson[45] Chapter 4.]

$$\dot{m}_{total} = A^* \cdot P_0 \cdot \sqrt{\frac{\gamma}{R_g \cdot T_0} \cdot \left( \frac{2}{\gamma + 1} \right)^{\frac{\gamma+1}{\gamma-1}}} . \tag{3}$$

The calculation of Eq. (2) assumes the flow composition is frozen at the nozzle entrance, (Anderson, [45], pp 659-661) and nozzle erosion during the burn.

A table of thermodynamic and transport equilibrium properties of the GOX/ABS, GOX/PMMA, HTP/ABS and HTP/PMMA exhaust plumes were calculated using the previously described CEA code[41] with chamber pressure $P_0$ and mean *O/F* ratio as independent look up variables for the tables. For each data point in the burn time history, the two-dimensional tables of thermodynamic and transport properties were interpolated using chamber pressure $P_0$ and mean *O/F* ratio as lookup variables. Calculated parameters included the gas constant $R_g$, ratio of specific heats $\gamma$, and flame temperature $T_0$. Defining the combustion efficiency as

$$\eta^* = \frac{c^*_{actual}}{c^*_{ideal}} = \frac{\sqrt{\left( \frac{\gamma+1}{2 \cdot \gamma} \right)^{\frac{\gamma+1}{(\gamma-1)}} R_g \cdot T_{0_{actual}}}}{\sqrt{\left( \frac{\gamma+1}{2 \cdot \gamma} \right)^{\frac{\gamma+1}{(\gamma-1)}} R_g \cdot T_{0_{ideal}}}} \approx \sqrt{\frac{T_{0_{actual}}}{T_{0_{ideal}}}} , \tag{4}$$

the theoretical flame temperature $T0_{ideal}$ was scaled by adjusting the combustion efficiency

$$T_{0_{actual}} = \eta^{*2} \times T_{0_{ideal}} , \tag{5}$$

such that the calculated fuel mass consumption

$$\Delta M_{fuel} = \int_0^t \left( \dot{m}_{total} - \dot{m}_{ox} \right) dt \tag{6}$$

matched the measured value from differences of the pre- and post-test weight measurements. As described earlier, the consumed fuel mass anchored the thermodynamic calculations.

Adjusting input combustion efficiency upwards has the effect of increasing the calculated fuel mass consumption, and downwards decreases the calculated fuel mass consumption. The calculations of Equations (3-6) were iterated, adjusting $\eta^*$ after each iteration, until the calculated fuel mass matched the measured mass within a prescribed level of accuracy, in this case 0.5%. For each iteration, the time-averaged *oxidizer-to-fuel* ratio was calculated as integrated oxidizer massflow divided by the consumed fuel mass,

$$\overline{O/F} = \frac{\int_0^{t_{burn}} \dot{m}_{ox}(t)\cdot dt}{\Delta M_{fuel}} = \frac{\int_0^{t_{burn}} \dot{m}_{ox}(t)\cdot dt}{\int_0^{t_{burn}} \left[\dot{m}_{total}(t) - \dot{m}_{ox}(t)\right]\cdot dt} \quad (7)$$

***Calculating the Motor Performance Parameters***

The 1-dimensional de Laval flow equations (Anderson [45], Chapter 4) were used to calculate the thruster performance parameters. Thrust and thrust coefficient were calculated from chamber pressure as

$$F_{thrust} = P_0 A^* \cdot \left( \sqrt{\frac{2}{\gamma-1}\cdot\left(\frac{2}{\gamma+1}\right)^{\frac{\gamma+1}{\gamma-1}}\left(1-\frac{p_{exit}}{P_0}\right)^{\frac{\gamma-1}{\gamma}}} + \left(\frac{A_{exit}}{A^*}\right)\left(\frac{p_{exit}-p_\infty}{P_0}\right) \right), \quad (8)$$

$$C_F = \frac{F_{thrust}}{P_0 A^*} = \gamma\sqrt{\frac{2}{\gamma-1}\cdot\left(\frac{2}{\gamma+1}\right)^{\frac{\gamma+1}{\gamma-1}}\left(1-\frac{p_{exit}}{P_0}\right)^{\frac{\gamma-1}{\gamma}}} + \left(\frac{A_{exit}}{A^*}\right)\left(\frac{p_{exit}-p_\infty}{P_0}\right) \quad (9)$$

Specific Impulse, Characteristic Velocity, and Impulse density were calculated as

$$I_{sp} = \frac{F_{thrust}}{g_0 \dot{m}_{total}}, \quad c^* = \frac{P_0 \cdot A^*}{\dot{m}_{total}}, \quad \rho I_{sp} = s_g \cdot g_0 \cdot I_{sp} \quad (10)$$

In Eq. (10) $g_0$ is normal acceleration of gravity at sea level, *9.8067 m/s²*. The thrust coefficient $C_F$ and specific impulse $I_{sp}$ were also calculated directly from the thrust sensed by the test stand load cell. Values calculated from both sources will be presented later in order to support the verisimilitude of the collected test data.

## EXPERIMENT SETUP

The test apparatus and motor configuration for the tests presented in this paper are portrayed in this section.

### *Test Article*

Figure 7 and Figure 8 shows the motor configuration, which includes the injector cap containing a COTS spray injector nozzle, 38mm motor casing, ignition cap, fuel grain, and 1N nozzle retainer assembly. The motor case was machined from 316-grade stainless steel. The injector cap, which includes ports for the injector, ignition electrodes and chamber pressure fitting, was machined from 6061-T6 grade aluminum. The nozzle was machined from a single piece of graphite. The spark cap is printed separately from the fuel grain to ensure that the catalyst infusion does not inhibit the arcing capabilities of the ABS to achieve a strong spark for ignition.

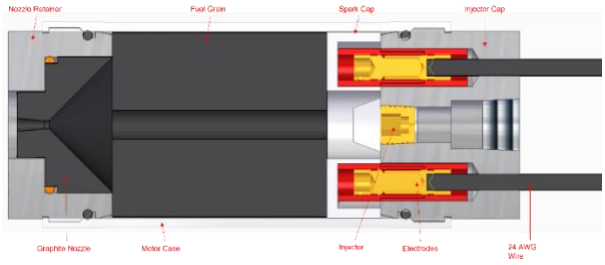


**Figure 7: Motor Assembly**

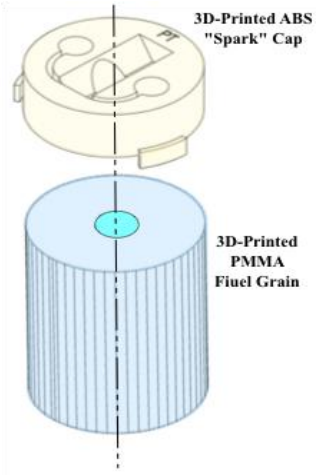


**Figure 8: CatGrain with ABS Spark Cap**

### *Test Apparatus*

Figure 9 and Figure 10 show the test cart used for the tests conducted and the system Piping and Instrumentation diagram associated with the layout of the cart. The system is pressurized with Nitrogen gas ($N_2$) or GOX to dictate HTP flow rates. A separate path for $N_2$ leads directly to motor injection to provide a fire suppression and purge function in the case of a misfire.

Fire control and data acquisition are managed from outside the test cell using laptop computer that communicates with the instrumentation system via a single Ethernet Bus. The GOX and HTP valves and ignition system are powered separately through arming switches, giving each system a “safe” and “armed” state to eliminate the possibility of accidental ignition. Motor performance measurements include motor injector and chamber pressure, and thrust level is sensed by a load cell mounted to the test sled.

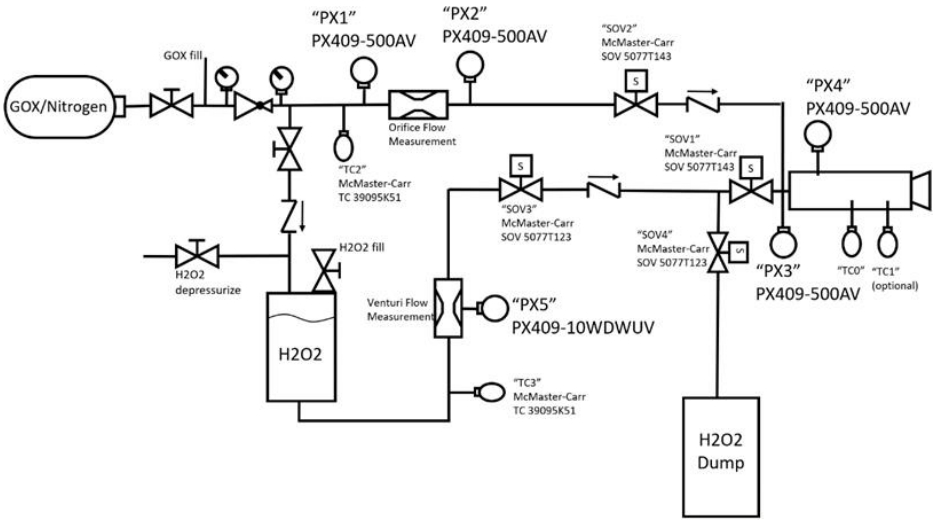


**Figure 9. HTP Hybrid Thruster Test System Piping and Instrumentation Diagram.**

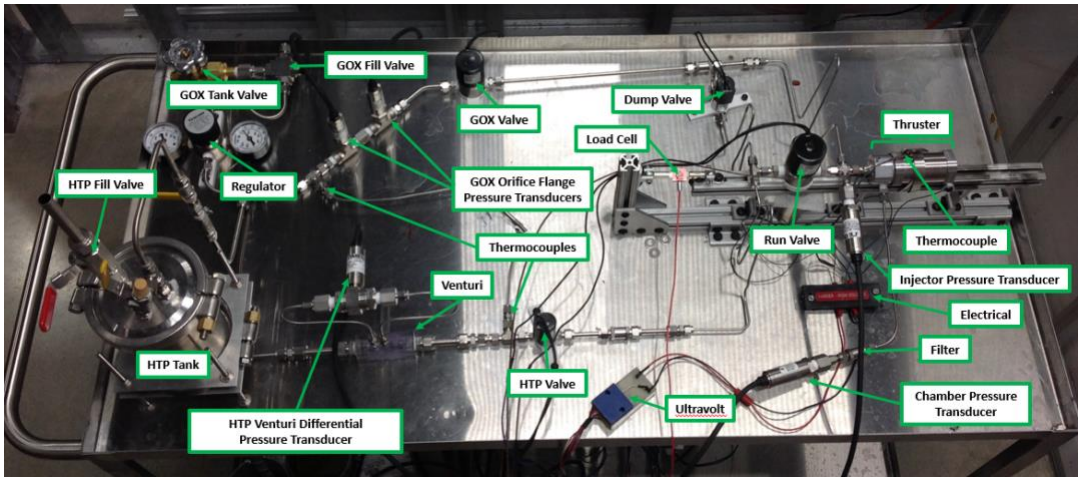


**Figure 10. Thruster Mounted on Test Cart.**

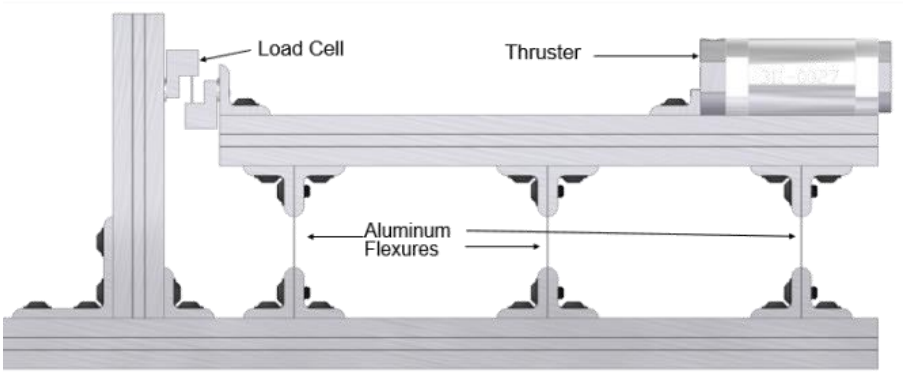


**Figure 11. Motor Sled with Mounted Thrust Chamber and Load Cell.**

The thruster chamber is mounted on an inverted pendulum thrust stand. This consists of an aluminum T-slot railing supported by three thin aluminum flexures. These flexures allow the structure to move in the direction of the thrust axis when the motor fires, resulting in load cell measurements. Figure 11 shows this mounting configuration. The motor fires to the right of the test sled in this image.

### *CatGrain Fabrication*

The catalyst-infused fuel grain (CatGrain) is critical to the development of an HTP propulsion system that can be a simple drop-in replacement of a GOX propulsion system without ignition latency or increased ignition energy.

The CatGrain is created by diffusing a potassium permanganate ($KMnO_4$) catalyst solution into a fuel grain. To achieve sufficient diffusion, the fuel grain material must be porous. Most fuel grains used for hybrid rocket motors are plastic, which are not porous enough – if at all – as extruded or cast material. Plastic filament used for FDM 3D printing is porous, and the layering in printed parts provides additional locations for diffusion. Printed ABS is the best choice for this application because of the porosity and burn characteristics with HTP. Figure 12 shows the ABS fuel grain before and after KMnO4 infusion.

**Figure 12: ABS Fuel Grain Before (left) and After (right) Catalyst Infusion**

The chemical reaction between $KMnO_4$ and HTP is

$$3H_2O_2 + 3KMnO_4 \rightarrow 3O_2 + 2MnO_2 + KOH + 2H_2O$$

Although $KMnO_4$ is not a true catalyst for HTP ($KMnO_4$ reduces to Manganese Oxide ($MnO_2$) as a purer catalyst form as shown in Equation 14), $MnO_2$ is not soluble in a solution that does not break down ABS plastic, whereas $KMnO_4$ is soluble. Noble metals like platinum or silver are also not considered for the same reason as $MnO_2$ and also because noble metals are orders of magnitude more expensive. For convenience and simplicity, water is used as the solvent for the catalyst solution.

## RESULTS AND DISCUSSION

This section presents preliminary results from the initial testing campaign. To date, a total of 14 successful full-combustion CatGrain hot firings have been performed.

### *Validation Tests*

From the initial validation tests conducted, the CatGrain shows strong promise, with initial test data shown in Figure 14. A rise time of 1.3 seconds is observed, with average steady-state ambient Isp and c* performance values at 177 seconds and 1234 m/s, respectively. The O/F ratio is lower than ideal. This is due to the $KMnO_4$ increasing combustion pressure more than a similar setup with a non-catalyzed ABS fuel grain typically achieves[46], which reduces the pressure-fed HTP injection, resulting in a fuel rich combustion environment. Additionally, the increase in chamber pressure also increased the generated thrust.

Core burning hybrid motors are susceptible to an O/F ratio shift during the burn, especially the first several seconds of the initial burn when the combustion port area changes most rapidly. This is evident in this test, where the O/F ratio starts at around 2 but decays down to 1 over the 15 second hot-fire. The result is a less stoichiometric burn, yielding lower thrust and therefore reduced performance than the theoretical peak. Despite this, the performance attained from this initial test shows the potential for this system to match and outperform hydrazine and its newer "green" derivatives.

For comparison, a test with a normal ABS fuel grain – not a CatGrain – was conducted. The results are shown in Figure 13. A significant rise time is seen, about 5.02 seconds. Because there was so short of time of actual combustion, there was very little mass burned. As such, the calculations presented in Data Analysis Methods Section to calculate the fuel massflow and subsequent performance data could not be sufficiently anchored by the measured fuel burned. Thus, performance data is not presented, only the measured thrust.

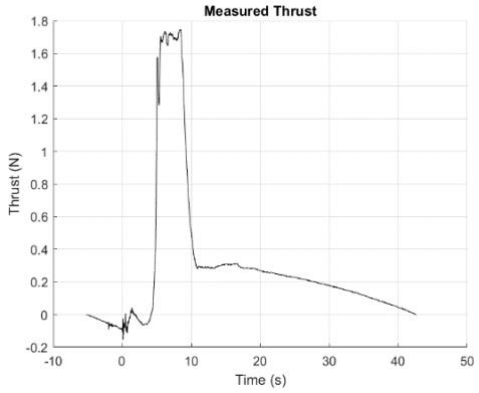


**Figure 13: Hot Fire of Extruded ABS Fuel Grain**

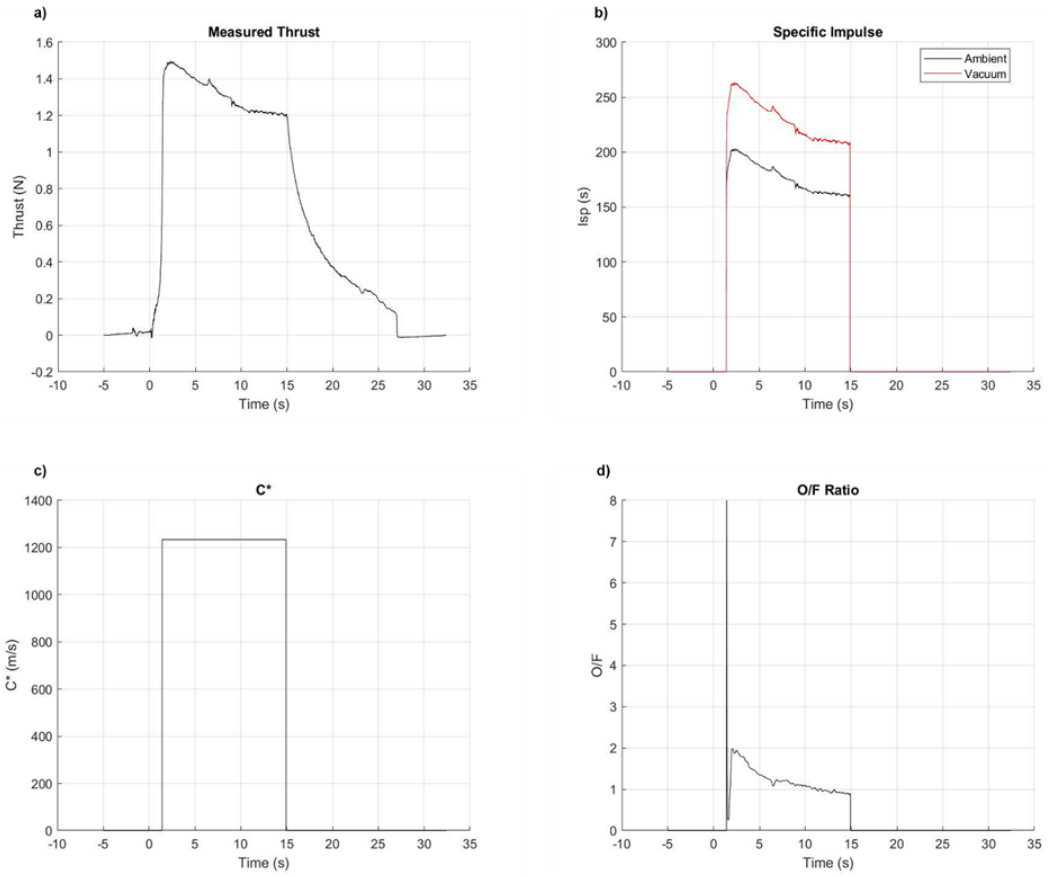


**Figure 14. Test Data of Initial CatGrain Performance Test**

***Re-ignition Tests***

An issue that results from the low O/F ratio is the difficulty to reignite the CatGrain without needing to re-dope the surface with more KMnO4. The low O/F ratio produces a "dirtier" burn, leaving a significant amount of soot deposited on the burned surface. This inhibits the ability for the infused catalyst to directly contact HTP upon injection to release GOX to aid in ignition. Additionally, the "erosive burning" prevalent with an atomizing spray injector reported by Smith[46] eventually burns away portions of the ignition cap, which eliminates the electrical path after extended burns.

Several configurations were explored to prevent the spray injection from burning away the spark cap while also maintaining a source of unburned and soot-free catalyst to provide the GOX release necessary for reliable ignition.

*Boron Nitride Ignition Cap Insulation*

One method tested was to redesign the spark cap in a way that insulates the ABS ignition fuel with a high-temperature ceramic, shown in Figure 15. Boron-Nitride was selected due to its high thermal resistance and being a porous ceramic. The porosity allowed for the BN insulator to absorb KMnO4 and provide an additional source of HTP decomposition for GOX release for ignition.

Though this did work for the first hot fires, this method did not work long-term. The small geometry associated with this size of motor resulted in the ceramic insulator fracturing from the pressure and thermal shock, sending fragments down the chamber and clogging the nozzle.

**Figure 15: Boron-Nitride-Insulated Spark Cap Design (left) and Fracturing Post-Burn (right)**

*Alumina Tape Ignition Cap Insulation*

The boron-nitride insulator was too brittle, a ceramic tape cloth was employed, shown in Figure 16. A high-temperature alumina tape with a temperature rating to 1700 C was also infused with KMnO4, formed into a small ring, and secured to the walls of the inner opening of the spark cap. This method worked better, but unfortunately was still partially consumed where the cloth meets the fuel grain combustion region, indicating the point where combustion temperatures reach above 1700 C. This provided successful insulation for the electrodes of the spark cap but did not allow for maintaining unconsumed KMnO4 where it would directly impinge with HTP to release GOX for ignition.


**Figure 16: CatGrain and Spark Cap with Ceramic Tape**

*Stainless Steel Wire Mesh*

Keeping the alumina tape insulation to protect the electrodes was still useful, but an additional component is needed to provide the catalyst support that will not be consumed or coated by soot. A stainless steel wire mesh disc was chosen, first tested with a gridded mesh of 20x20 holes per one square inch. The mesh was impregnated with KMnO4, then calcined in a furnace at 600 C for 2 hours to burn away the potassium and yield a manganese oxide (MnO2) deposit, which is a true catalyst for HTP. This means that there is no redox reaction like there is with KMnO4 and thus should not be reduced with the volume of HTP being passed through the mesh.

The 20x20 mesh grid was chosen to allow for some HTP to contact with impregnated mesh while some to pass through undecomposed. The mesh is placed on top of the spark cap, coming in direct contact with the injector exit, shown in Figure 17. This configuration yields a "staged decomposition" by having multiple points for initial decomposition of fractions of the HTP volume before sustained combustion is reached.

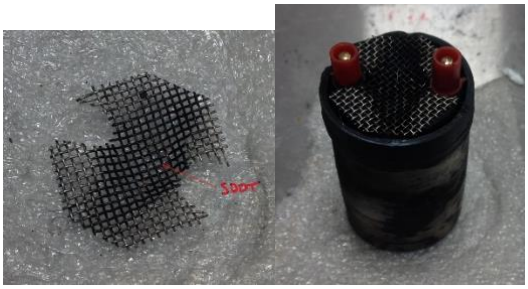

**Figure 17: Stainless Steel 20x20 Grid Mesh Post-Fire**

This method proved quite effective, as the physical separation from the combustion region within the CatGrain helped reduce the buildup of soot, though not completely eliminate it. Upon inspection post-fire, there was still small amounts of soot coating the mesh, seen in Figure 17. However, when the soot coating was brushed off and a drip test was performed on the mesh, it demonstrated a retention in strong catalytic activity, proving the importance of calcining the KMnO4 to yield MnO2.

To reduce the soot buildup, the O/F ratio must increase. The best option to accomplish this is to reduce the length of the CatGrain. Tests with a reduced length CatGrain are yet to be done and as such not presented in this paper.

*Nickel Foam*

Though the stainless steel mesh method showed initial success, the nature of this material does not allow for much infusion of catalyst into the steel. A thin metal foam sheet would provide a better structure to support more catalyst material, potentially further improving the ignition latency. Nickel foam was chosen because it has a higher melting temperature and is cheaper to produce.

The pore density of metal foam absorbed more catalyst, yielding about 10% MnO2 as compared to 2.5% for the stainless steel mesh. The increased pore density proved to not be useful, as it slowed down the oxidizer flow slightly and also served to push some HTP more radially, increasing the erosive burning on the spark cap.

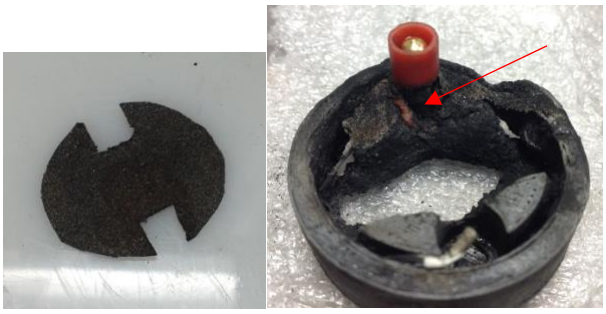

**Figure 18: Nickel Foam (left) and Resulting Erosion Burn (right)**

To avoid the reduction in oxidizer flow through the nickel foam, several small holes were drilled through the center to act more like the wire mesh, where some peroxide could pass through unobstructed and undecomposed, shown in Figure 19. This modification drastically improved the ignition latency down to 0.741 seconds, shown in Figure 20, though didn't fully get rid of the radial flow issue. Additionally, the nickel foam material was only 0.3 mm thick, which ended up getting burned through, seen in Figure 21, preventing use for re-ignition. This is likely from erosion burning from the HTP instead of the actual combustion temperature in the chamber. A thicker foam would survive better but may not allow for staged decomposition. This has yet to be tested.

From these findings, there appears to be an optimal spacing or pore size for the staged decomposition ignition method while retaining structure and catalyst to attain re-ignition. More configurations and tests are to be conducted investigating this hypothesis.

**Figure 19: Nickel Foam with MnO2 and Drilled Pass-Through Holes**

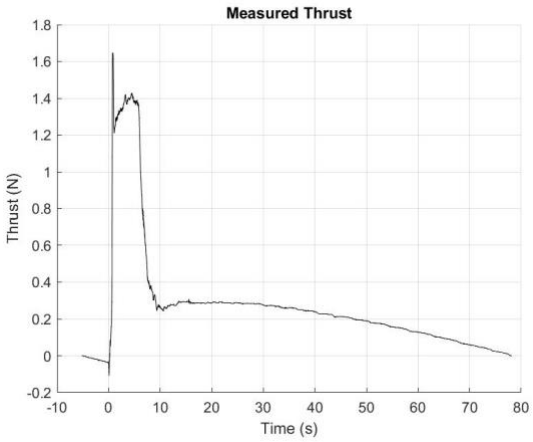


**Figure 20: Measured Thrust of CatGrain and Nickel Foam with Pass-Through Holes**

**Figure 21: Burned Out Nickel Foam**

***Reliability***

The last 10 tests have all successfully achieved ignition, with ignition latencies and associated ignition methods reported in Table 1. To date, re-ignition has not reliably been proven, largely due to having burns that are too fuel rich that leave soot deposits within the chamber. CatGrains that were burned more than once were ignited with a new alumina tape or metal mesh. Re-ignition reliability is expected to be attained with an optimized grain geometry for the next upcoming tests.

**Table 1: Latest Tests with Rise Time and Configuration**

| Date | Rise Time (seconds) | Configuration |
|---|---|---|
| 3/23/2023 | 1.6 | CatGrain4 with Boron Nitride |
| 4/6/2023 | 1.859 | CatGrain5 with Alumina Tape |
| 4/17/2023 | 3.549 | CatGrain6 with Alumina Tape |
| 4/26/2023 | 1.503 | CatGrain6 with Alumina Tape |
| 5/3/2023 | 1.481 | CatGrain6 with Alumina Tape |
| 5/19/2023 | 1.242 | CatGrain8, Alumina Tape, SS Mesh |
| 5/19/2023 | 0.926 | CatGrain8, Alumina Tape, SS Mesh |
| 5/30/2023 | 1.87 | CatGrain10, Nickel Foam |
| 5/30/2023 | 0.741 | CatGrain10, Alumina Tape, Nickel Foam |
| 5/30/2023 | 0.616 | CatGrain10, Alumina Tape, Nickel Foam |

***Performance***

The "CatGrain" system was used as a true “drop-in” replacement, allowing HTP to be burned directly in the legacy 1-N GOX/ABS HPGHP thruster with no hardware modifications. However, because of the longer aspect ratio associated with the legacy GOX/ABS thrust chamber, the resulting O/F ratios for HTP/CatGrain were well-below the optimal point for HTP combustion; thus, the associated specific impulse values are lower than would be achieved for an optimized geometry, varying between 170 and 185 seconds. Assuming a high expansion ratio nozzle (25:1), these values extrapolate to between 225-250 seconds for vacuum specific impulse,

**SUMMARY AND CONCLUSION**

In support of the emerging SmallSat market, there does not currently exist a Commercial Off the Shelf (COTS) "green" propulsion system that offers both intermediate thrust and specific impulse levels in the 240-300 second range. The only available options are associated with gold-gas flow or monopropellant hydrazine. Cold-gas systems are volumetrically inefficient and produce very low $I_{sp}$. Hydrazine-based systems bring a wide range of objective and environmental hazard issues, and their use can significantly increase operating costs of the total spacecraft system.

To fill this technology gap, SDL and PRL-USU have partnered to develop a non-toxic hybrid prototype propulsion system based on Utah State's HPGHP. HPGHP technology leverages the unique dielectric breakdown properties of 3D printed ABS to develop family of hybrid propulsion systems with capability for reliable start, stop, and re-ignition.

In its most mature form, the HPGHP system uses GOX as the oxidizer. Unfortunately, unless stored at very high pressures, GOX has a low specific gravity and is a volumetrically inefficient propellant. Due to its high density and excellent oxidizing performance, HTP was considered to be very promising alternative "drop-in" oxidizer for this application.

Although HPGHP ignition works quite reliably with GOX as the oxidizer, the technology has experienced reliability and ignition latency issues when GOX is replaced by HTP. Although catalytic decomposition works well for monopropellant hydrogen peroxide systems, for hybrid systems the resulting enthalpy levels due to catalytic decomposition are often too low to achieve full combustion, and ignition is highly unreliable.

An alternative method, as tested in this study, replaces the external catalyst by diffusion-blending ABS with 1-2% potassium permanganate ($KMNO_4$), and then 3-D printing fuel grains using the augmented feed-stock. The embedded catalyst allows for near-instantaneous decomposition as HTP enters the combustion chamber, releasing gaseous oxygen that, when combined with the arc-ignition energy, provides quick and reliable ignition. No preheat is required, and the infused fuel does not reduce the overall system performance.

The "CatGrain" system was used as a true “drop-in” replacement, allowing HTP to be burned directly in the legacy 1-N GOX/ABS HPGHP thruster with no hardware modifications. However, because of the longer aspect ratio associated with the legacy GOX/ABS thrust chamber, the resulting O/F ratios for CatGrain thruster were well-below the optimal point for HTP combustion; thus, the associated specific impulse values are lower than would be achieved for an optimized geometry.

Even with the non-optimal thrust chamber geometry, the GatGrain/HPGHP configuration still out-performs monopropellant hydrazine and the ionic-liquid “green” hydrazine alternatives. There are clear steps that can be taken to improve the O/F ratio of this CatGrain hybrid motor, starting with shortening the fuel grain length.

The ignition method was enhanced by adding a metal mesh between the injector and spark cap that is coated in MnO2, providing a “staged decomposition” effect that showed a measurable reduction in ignition latency from an average of 1.5 seconds to less than 1 second. Re-ignition has not yet been achieved with this system because of the buildup of soot on the metal meshes, which inhibits the instantaneous reaction of HTP contacting $MnO_2$.

Despite this issue, there is proven reliability in achieving initial ignition using this configuration. Additionally, it is hypothesized that with more O/F optimization the soot buildup will be resolved, allowing the MnO2 coated mesh to continuously provide the stage decomposition effect over the lifetime of the motor and thus have reliable re-ignition.

***Acknowledgments***

The authors would like to thank the Space Dynamics Lab for providing testing facilities used to gather the data reported in this paper. The authors also want to thank the NASA Small Spacecraft Technology Program (SSTP) for partially funding this work through the Cooperative Agreement (CA) Partnerships with Universities and NASA Centers, Grant No. 80NSSC20M0083.

**REFERENCES**


1. Choudhary, G., Hansen, H., Donkin, S., and Kirman, C., "Toxicological Profile for Hydrazines," Vol. 21, U.S. *Dept. of Health and Human Services*, Public Health Service, Agency for Toxic Substances and Disease Registry, 1997, pp. 1–224. https://www.atsdr.cdc.gov/toxprofiles/tp100.pdf

2. Bombelli, V., "Economic Benefits for the Use of Non-toxic Monopropellants for Spacecraft Applications, AIAA-2003-4783, [39th AIAA/ASME/SAE/ASEE Joint Propulsion Conference and Exhibit, Huntsville, AL, July 2003.] https://doi.org/10.2514/6.2003-4783

3. Haeseler, D., Bombelli, V., Vuillermoz, P., Lo, R., Marée, T., & Caramelli, F., "Green Propellant Propulsion Concepts for Space Transportation and Technology Development Needs," ESA SP-557, [Proceedings of the 2nd International Conference on Green Propellants for Space Propulsion, Cagliari, Sardinia, Italy, 7-8 June 2004.] https://adsabs.harvard.edu/full/2004ESASP.557E...4H

4. Hawkins, T. W., Brand, A. J., McKay, M. B., and Tinnirello, M., "Reduced Toxicity, High Performance Monopropellant at the U.S. Air Force Research Laboratory," AFRL-RZ-ED-TP-2010-219, [4th International Association for the Advancement of Space Safety Conference, Huntsville, AL, 19-21 May 2010.] https://ui.adsabs.harvard.edu/abs/2010ESASP.680E..10H/abstract

5. Goldstein, Edward, "The Greening of Satellite Propulsion," *Aerospace America*, February, 2012, pp. 26-28. https://www.researchgate.net/publication/293560444_The_greening_of_rocket_propulsion

6. Larsson, A., and Wingborg, N., "Green Propellants Based on Ammonium Dinitramide (ADN)," *Adv. in Spacecraft Tech.*, Vol. 2, Intech Open, London, U.K., 2011, Chap. 7. https://doi.org/10.5772/13640

7. Patel, A., Zhang, Y., and Shashurin, A., "Liquid-Fed Pulsed Plasma Thruster with Low-Energy Surface Flashover Igniter for Propelling Nanosatellites," *J. of Prop. and Power*, Vol. 36, No. 5, Sept. 2020, pp. 715–720. https://doi.org/10.2514/1.B37800.

8. Amrousse, R., Katsumi, T., Azuma, N., Hatai, K., Ikeda, H., and Hon, K., "Development of Green Propellants for Future Space Applications," *Sci. and Tech. of Eng. Mat.*, Vol. 77, Nos. 5–6, 2016, pp. 105–110. http://www.jes.or.jp/mag/stem/Vol.77/documents/Vol.77,No.5,p.105-110.pdf

9. Pokrupa, N., Anglo, K., and Svensson, O., "Spacecraft System Level Design with Regards to Incorporation of a New Green Propulsion System," AIAA-2011-6129, [46th AIAA/ASME/SAE/ASEE Joint Propulsion Conference and Exhibit, San Diego, CA, July 31-Aug 3, 2011.] https://doi.org/10.2514/6.2011-6129

10. Nagamachi, M. Y., Oliveira, J. I., Kawamoto, A. M., and Dutra, R., C., "ADN – The new oxidizer around the corner for an environmentally friendly smokeless propellant," *J. of Aerospace Technology Management*, Vol. 1, No. 2., December 2009, pp. 153-160. http://dx.doi.org/10.5028/jatm.2009.0102153160

11. Persson, M., Anflo, K., and Dinardi, A., "A Family of Thrusters For ADN-Based Monopropellant LMP-103S," AIAA-2012-3815, [48th AIAA/ASME/SAE/ASEE Joint Propulsion Conference & Exhibit 30 July - 01 August 2012, Atlanta, Georgia, 2012.] https://doi.org/10.2514/6.2012-3815.

12. Ide, Y., Takahashi, T., Iwai, K., Nozoe, K., Habu, H., and Tokudome, S., "Potential of ADN-Based Ionic Liquid Propellant for Spacecraft Propulsion," *Procedia Engineering*, Vol. 99, 2015, pp. 332–337. https://doi.org/10.1016/j.proeng.2014.12.543

13. Dennis Meinhardt, D., Brewster, G., Christofferson, S., and Wucherer, E., "Development and testing of new, HAN-based monopropellants in small rocket thrusters, AIAA 90-4006. [34th AIAA/ASME/SAE/ASEE Joint Propulsion Conference and Exhibit, 13 July 1998 - 15 July 1998, Cleveland,OH,U.S.A.] https://doi.org/10.2514/6.1998-4006

14. Spores, R. A., Masse, R., and Kimbrel, S., "GPIM AF-M315E Propulsion System," [AIAA_2013-3849, [49th AIAA/ASME/SAE/ASEE Joint Propulsion Conference & Exhibit, San Jose CA, 15-17 July 2013.] https://doi.org/10.2514/6.2013-3849

15. Anflo, K.; Crowe, B. In-Space Demonstration of an ADN-based Propulsion System, [AIAA-2011-5832. [47th AIAA/ASME/SAE/ASEE Joint Propulsion Conference & Exhibit, San Diego, CA, USA, 31 July–03 August 2011]. https://doi.org/10.2514/6.2011-5832

16. Masse, R., Spores, R. A., Allen, M., Lorimer, E., Meyers, P, and McLean, C., "GPIM AF-M315E Propulsion System," [AIAA 2015-3753. [51st AIAA/SAE/ASEE Joint Propulsion Conference. July 2015.] https://doi.org/10.2514/6.2015-3753

17. McLean, C.; Marotta, B.; Porter, B. Flight performance of the propulsion subsystem on the green propellant infusion mission, AAS 20-062. [30th AIAA/AAS Space Flight Mechanics Meeting, Orlando, FL, USA, 6–10 January 2020]; http://www.univelt.com/AASPapers.html (Accessed on 25 May 2022).

18. Anflo, K.; Crowe, B. "In-Space Demonstration of an ADN-based Propulsion System," [AIAA-2011-5832.

[47th AIAA/ASME/SAE/ASEE Joint Propulsion Conference & Exhibit, San Diego, CA, USA, 31 July–03 August 2011.] https://doi.org/10.2514/6.2011-5832

19. Kang, S., and Kwon, S., "Difficulties of Catalytic Reactor for Hydroxylammonium Nitrate Hybrid Rocket," *Journal of Spacecraft and Rockets*, Vol. 52, No. 5, Sept.–Oct. 2015, pp. 1508–1510. https://doi.org/10.2514/1.A33255

20. Katsumi, T.; Hori, K. "Combustion Wave Structure of Hydroxylammonium Nitrate Aqueous Solutions," AIAA 2010-6900. [ 46th AIAA/ASME/SAE/ASEE Joint Propulsion Conference & Exhibit, Nashville, TN, USA, 25–28 July 2010.] https://arc.aiaa.org/doi/10.2514/6.2010-6900

21. Whitmore, S.A.; Burnside, C.G. Performance Analysis of a High Performance Green Propellant Thruster. NASA Marshall Space Flight Center Faculty Program, NASA TM-2015-218216. December 2015; pp. 125–151. Available online: https://ntrs.nasa.gov/search.jsp?R=20160000456 (Accessed on 1 December 2019).

22. Lowe, D. The Overselling of Ionic Liquids. Science Magazine, In The Pipeline, 11 June 2013. http://blogs.sciencemag.org/pipeline/archives/2013/06/11/the_overselling_of_ionic_liquids (Accessed on 24 May 2022).

23. Anon., "Hazard Analysis of Commercial Space Transportation; Vol. 1: Operations, Vol. 2: Hazards, vol. 3: Risk Analysis," U.S. Dept. of Transportation, PB93-199040, Accession No. 00620693, May 1988. https://rosap.ntl.bts.gov/view/dot/35788.

24. Anon., "Department of Defense Interface Standard, Electromagnetic Environmental Effects requirements for Systems, MIL-STD-464, http:// http://www.tscm.com/MIL-STD-464.pdf, [Accessed 24 May 2022].

25. "Electromagnetic Environmental Effects Requirements for Systems," United Sates Dept. of Commerce National Technical Information Service, Vol. MIL-STD-46, Springfield, VA, 2010. https://absolute-emc.com/article/MIL-STD-464

26. Sutton, G., and Biblarz, O., *Rocket Propulsion Elements, 9th ed*., Wiley, New York, 2016, Chaps. 15, 19. ISBN-13: 978-1118753651, ISBN-10: 1118753658.

27. Cheng, G., Farmer, R., Jones, H., and McFarlane, J., "Numerical Simulation of the Internal Ballistics of a Hybrid Rocket Motor," AIAA 1994-0554. [32nd Aerospace Sciences Meeting and Exhibit, , Jan. 1994.] https://doi.org/10.2514/6.1994-554

28. Whitmore, S. A., "Three-Dimensional Printing of "Green" Fuels for Low-Cost Small Spacecraft Propulsion Systems," Journal of Spacecraft and Rockets, Vol. 55, No. 1, 2018, pp. 13–26. https://doi.org/10.2514/1.A33782

29. Mathias, S. D., Whitmore, S. A., and Harvey, R., "High Voltage Breakdown and Arc-Tracking Mechanism of Thermoplastics with Applications to Hybrid Rocket Arc- Ignition," *AIAA 2017-4601, 53rd AIAA/SAE/ASEE Joint Propulsion Conference*, 10-12 July 2017, Atlanta, GA. https://doi.org/10.2514/6.2017-4601

30. Whitmore, Stephen A., "Additive Manufacturing as an Enabling Technology for "Green" Hybrid Spacecraft Propulsion," RAST-1039, *Conference on Recent Advances in Space Technology 2015*, Istanbul Turkey, June 16-19 2015. https://ieeexplore.ieee.org/document/7208305

31. Whitmore, S. A., Merkley, Stephen L., Zachary S., Walker, Sean D., "Development of a Power Efficient, Restartable, "Green" Propellant Thruster for Small Spacecraft and Satellites," SSC15-P-34, *29th AIAA/USU Conference on Small Satellites*, Logan UT, 8-13 August, 2015. https://digitalcommons.usu.edu/smallsat/2015/all2015/90/

32. Whitmore S. A., "Three-Dimensional Printing of "Green" Fuels for Low-Cost Small Spacecraft Propulsion Systems," *Journal of Spacecraft and Rockets*, Vol. 54, No. 6 (2017), https://doi.org/10.2514/1.A33782

33. Whitmore, S. A., Bulcher, A. M., Lewis, Z., and Inkley, N. "Methods and Systems for Restartable Hybrid Rockets," United States Patent 10,774,789 B2, September 15, 2020. https://patents.google.com/patent/US20150322892A1/en.

34. Whitmore, S. A., and Anthony M. Bulcher, A. M., "Vacuum Test of a Novel Green-Propellant Thruster for Small Spacecraft", AIAA 2017-5044. [5*3rd AIAA/SAE/ASEE Joint Propulsion Conference, AIAA Propulsion and Energy Forum*, 2017.] https://doi.org/10.2514/6.2017-5044

35. Whitmore, S. A., and Bulcher, A. M., "A Green Hybrid Thruster Using Moderately Enriched Compressed Air as the Oxidizer", AIAA 2018-4841, [*2018 Joint Propulsion Conference, AIAA Propulsion and Energy Forum*,] https://doi.org/10.2514/6.2018-4841

36. Rommingen, J. E., AND Husdal J., *"Nammo Hybrid Rocket Propulsion TRL Improvement Program,"* AIAA-2012-4311 [48th AIAA/ASME/SAE/ASEE Joint Propulsion Conference & Exhibit; 2012.] https://doi.org/10.2514/6.2012-4311

37. Whitmore S. A., Merkley D. P., "Arc-Ignition of an 80% Hydrogen Peroxide/ ABS Hybrid Rocket System," AIAA-2017-5047. [53rd AIAA/SAE/ASEE Joint

Propulsion 53rd AIAA/SAE/ASEE Joint Propulsion Conference, AIAA Propulsion and Energy Forum, Salt Lake City UT, July 10-14 2017.] https://doi.org/10.2514/6.2017-5047

38. Whitmore, S. A., and Martinez, C J., " Novel Catalyst Materials for Reducing Combustion Latency of a Thermally-Ignited Peroxide/ABS Hybrid Rocket," AIAA-2018-4445. [2018 AIAA Propulsion and Energy Forum Duke Energy Center Cincinnati Oh, 8-11 July, 2018.] https://doi.org/10.2514/6.2018-4445

39. Whitmore, S. A., and Martinez, C J., "Catalyst Development for an Arc-ignited Hydrogen Peroxide/ABS Hybrid Rocket System," Aeronautics and Aerospace Open Access Journal, MedCrave International, Vol. 2. No. 6, 2018, pp.356-388. https://medcraveonline.com/AAOAJ/catalyst-development-for-an-arc-ignited-hydrogen-peroxideabs-hybrid-rocket-system.html

40. Whitmore, S. A. "Direct Ignition of a High Performance Hydrogen Peroxide Hybrid Rocket with 3-D Printed Fuel," *Int. J. Astronaut. Aeronautical. Eng*., Vol. 4, No. 021, 2019). https://www.vibgyorpublishers.org/content/ijaae/fulltext.php?aid=ijaae-4-021

41. Gordon, S.; McBride, B.J., "Computer Program for Calculation of Complex Chemical Equilibrium Compositions and Applications," *NASA Technical Report RP-1311*; 1994. Available online: https://ntrs.nasa.gov/archive/nasa/casi.ntrs.nasa.gov/19950013764.pdf. (Retrieved on 22 May 2022).

42. Whitmore, S. A., and Merkley, S., "Radiation Heating Effects on Oxidizer-to-Fuel Ratio of Additively Manufactured Hybrid Rocket Fuels," *J. of Prop. and Power*, Vol.35, No. 4, 2019, pp. 863-878, https://arc.aiaa.org/doi/abs/10.2514/1.B37037

43. Smith, T. K., Lewis, Z. Olsen, K., Bulcher, M. A., and Whitmore, S. A., "A Miniaturized, Green, End-Burning, and Sandwich Hybrid Propulsion System," J. Prop. and Power, Published Online, May 2022, https://doi.org/10.2514/1.B38623

44. Karabeyoglu, A., Stevens, S., and Cantwell, B., "Investigation of Feed System Coupled Low Frequency Combustion Instabilities in Hybrid Rockets," AIAA 2007-5366. [43rd AIAA/ASME/SAE/ASEE Joint Propulsion Conference & Exhibit 8 - 11 July 2007, Cincinnati, OH.] https://doi.org/10.2514/6.2007-5366

45. Anderson, J. D. Jr., *Modern Compressible Flow with Historical Perspective*, *4th ed*., McGraw-Hill, New York, 2003, pp. 127–187. ISBN-13: 978-1260588767, ISBN-10: 1260588769.

46. Smith, T. K., Lewis, Z., Olsen, K., Thibaudeau, R., Whitmore, S.A., "A Miniaturized Hydrogen Peroxide/ABS Based Hybrid Propulsion Systems for CubeSats," AIAA/Utah State University Conference on Small Satellites, Logan, UT, 2022. https://digitalcommons.usu.edu/smallsat/2022/all2022/116/